Eur. Phys. J. B **45**, 97–102 (2005)
DOI: 10.1140/epjb/e2005-00168-5

THE EUROPEAN PHYSICAL JOURNAL B

Influence of Ni content on the microstructure and magnetic and magneto-optical properties of sputtered $(Co_{1-x}Ni_x)Pt_3$ alloy films

Z.Q. Zou[1,a], H. Wang[1], J. Zhou[2], D.F. Shen[2], and Y.P. Lee[3]

[1] Instrumental Analysis Center, Shanghai Jiaotong University, 1954 Huashan Road, Shanghai 200030, China
[2] Shanghai Institute of Metallurgy, Chinese Academy of Sciences, 865 Changning Road, Shanghai 200050, China
[3] Department of Physics, Hanyang University, Seoul 133-791, Korea

Received 15 February 2005
Published online 16 June 2005 –

Abstract. Influence of Ni content on the microstructure and magnetic and magneto-optical (MO) properties of sputtered $(Co_{1-x}Ni_x)Pt_3$ alloy films has been investigated by means of Kerr spectrometer, Kerr hysteresis looper, X-ray diffractometer (XRD), and atomic force microscopy (AFM). On the whole, the addition of Ni to the $CoPt_3$ alloy film simultaneously decreases the Curie temperature T_C and the Kerr rotation angle θ_K, but the decrease of T_C with Ni content is more visible. When the Ni content x is increased from 0 to 0.33, T_C decreases from 273 °C to 233 °C, whereas the decrease of θ_K is quite limited and the film still preserves a strong perpendicular magnetic anisotropy (PMA) and a high coercivity, indicating that the $(Co_{1-x}Ni_x)Pt_3$ alloy film with $x = 0.33$ can be used for practical MO applications. Further increase of Ni content decreases the θ_K significantly and destroys the PMA. XRD and AFM studies show that adding a small amount of Ni in the $CoPt_3$ alloy film will promote the growth of grains and roughen the film surface, and thus enhance the coercivity of the film. We observe also that both the coercivity and PMA are not sensitive to the (111) preferred orientation of the $(Co_{1-x}Ni_x)Pt_3$ alloy films.

PACS. 75.70.Ak Magnetic properties of monolayers and thin films – 75.50.Ss Magnetic recording materials – 85.70.Sq Magnetooptical devices

1 Introduction

During the past fifteen years, Co/Pt multilayers [1–3] and Co_xPt_{1-x} alloy films [4–8] have attracted much attention as possible candidates for the high-density perpendicular magnetic recording media and the next generation magneto-optical (MO) recording media, since they exhibit good corrosion resistance and superior magnetic and MO characteristics, such as strong perpendicular magnetic anisotropy (PMA), high coercivity, and large Kerr rotation at blue wavelengths. The PMA in Co/Pt multilayers is thought to originate from the anisotropy energy of the interface between Co and Pt layers, whose thicknesses are usually $2 \sim 4$ Å and about 10 Å, respectively, and is relatively easy to be weakened by the interlayer mixing caused by the repeated writing/erasing [4]. Hence, Co_xPt_{1-x} alloy films are more promising for applications in aspects of easy manufacturing and better thermal stability. In spite of this, a low Curie temperature T_C is still desirable for the MO storage media because of the high write sensitivity and high write/erase cyclability it provides. The practical disk writing temperatures attainable with low-cost laser sources today are between 150 and 200 °C [9]. However, the Co contents of Co_xPt_{1-x} alloy films with 100% perpendicular remanence, large PMA, and high coercivity were reported to be in the range of about $0.2 \sim 0.4$ at.% [5,6], and the corresponding Curie temperatures are between 200 and 415 °C [5,10], which are high for practical applications. Therefore, developing an approach to reduce the T_C while maintaining other advantages is desirable for practical uses. Because Ni-Pt alloy system is similar to Co-Pt in structure, lattice constant, and the polarizability of Pt [11], and the magnetization of bulk nickel (484 emu/cc) is much lower than that of bulk cobalt (1422 emu/cc) [9], the partial substitution of Ni for Co in the Co_xPt_{1-x} alloy film is a promising way to realize the purpose. Magnetic phase diagram also shows that the T_C of Co-Ni alloy will decrease significantly with the Ni content.

Experimentally, Ha et al. [12] reported that the T_C of Pd/Co multilayers could be reduced by the addition of Ni in the Co layers with a concentration of $0 \sim 0.53$ at.% while maintaining a large PMA energy. Hashimoto [13] found that the addition of Ni into the Co layer of the Co/Pt multilayers reduced the T_C without significant

[a] e-mail: zqzou@sjtu.edu.cn

decrease in the polar Kerr rotation and PMA, and the (Co, Ni)/Pt disk achieved a write/erase cyclability of about ten times higher than that of the Co/Pt disk under a constant carrier-to-noise ratio. Hence, it is expected that by alloying Ni with Co the T_C of the $Co_{1-x}Pt_x$ alloy films can be reduced or tailored to suit some special applications. In this article, we present an investigation on the dependence of microstructure and magnetic and MO properties of $(Co_{1-x}Ni_x)Pt_3$ alloy films on the Ni concentration.

2 Experiment

$(Co_{1-x}Ni_x)Pt_3$ alloy films were deposited on glass substrates by dc magnetron sputtering using a composite target with small Co and Ni chips pasted on a Pt disk. The area ratio of Co and Ni chips to the Pt disk was about 1 : 3. The atomic ratio of Ni to Co of the film, x, was adjusted by varying the area ratio of the Ni chips to the Co chips, and confirmed by Rutherford backscattering spectroscopy and a JCXA-733 electronic probe microanalyzer. The chamber was evacuated below 3×10^{-4} Pa before sputtering. 99.999% Ar was used as the working gas. During sputtering, the substrate was heated to 280 °C and the sputtering pressure was about 6 Pa, which turn out to be the optimal preparation conditions for the excellent magnetic and MO properties [6]. The film thickness was estimated from the deposition time and the deposition rate calibrated with a profilemeter. In this work, the thickness of all the films was kept at 72 nm.

The spectra of the saturated Kerr rotation and ellipticity of the samples were measured by a spectroscopic ellipsometer under a maximum magnetic field of 10 kOe perpendicular to the film plane at room temperature. A 150 W Xe short-arc lamp was used as a continuum light source to cover the spectral range of $1.5 - 4.5$ eV. The coercivity and Kerr rotation angle were obtained from the polar Kerr hysteresis loop measured at a wavelength of 633 nm (1.96 eV). Crystal structures of the films were analyzed by an X-ray diffractometer (XRD) using Cu K_α radiation ($\lambda = 1.54056$ Å). The Curie temperatures were determined by the Hall method described in references [14] and [15]. Surface micrographs of the films were obtained by an atomic force microscopy (AFM) (Auto-Probe CP Multitask System, Park Scientific Instruments).

3 Results and discussion

The polar Kerr rotation θ_K and the Curie temperature T_C for the films are essentially proportional to the magnetization of material. It is expected that partial substitution of Ni for Co in the $CoPt_3$ alloy film will reduce the magnetization, and thus depress the polar Kerr rotation and the Curie temperature. This can be interpreted in terms of the smaller Co-Ni and Ni-Ni exchange interactions as compared to the Co-Co exchange interaction, and the possible antiferromagnetic interaction among the transition metal atoms in the pseudobinary $(Co_{1-x}Ni_x)Pt_3$ disordered system [16–19]. Figure 1 shows the spectra of the

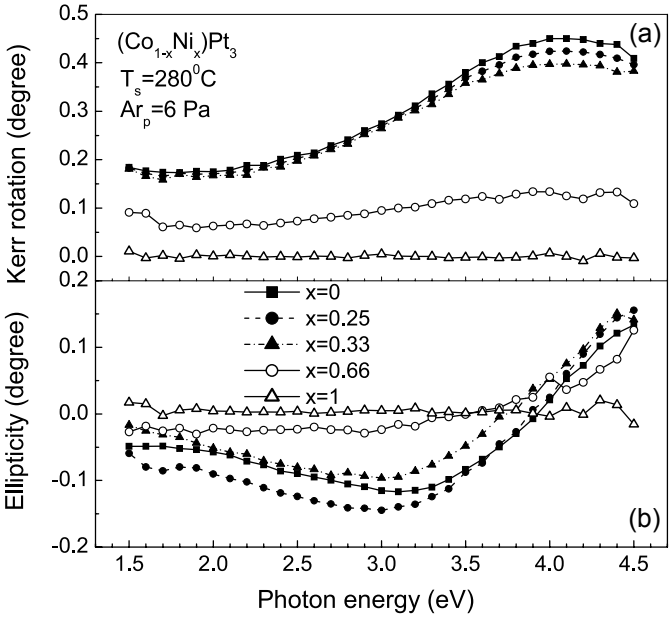

Fig. 1. (a) polar Kerr rotation θ_K and (b) ellipticity η_K spectra of the $(Co_{1-x}Ni_x)Pt_3$ alloy films with different Ni contents: $x = 0, 0.25, 0.33, 0.66$, and 1. The films are sputtered at 6 Pa and 280 °C.

polar Kerr rotation θ_K and ellipticity η_K in the range of $1.5 - 4.5$ eV for the $(Co_{1-x}Ni_x)Pt_3$ alloy films with $x = 0, 0.25, 0.33, 0.66$, and 1. At the lowest photon energy 1.5 eV (wavelength 826.6 nm), the Kerr rotations of the alloy films with $x = 0, 0.25$, and 0.33 are 0.184, 0.183, and 0.181°, respectively. With the increase of photon energy, the Kerr rotations decrease slightly at first, then increase monotonously until reaching respective maxima of 0.45, 0.42, and 0.398° at about 4.0 eV (wavelength 310 nm), and finally decrease slightly. It can be seen that in the whole detected photon energy range, θ_K decreases with increasing Ni content. However, the decrease is small when the Ni content x is less than 0.33, especially in the low photon energy region. Thereafter, the θ_K begins to decrease rapidly with increasing Ni content. At $x = 0.66$, the maximum of θ_K decreases to 0.134°, which is about one third of that of the $CoPt_3$ alloy film. At $x = 1$, both the polar Kerr rotation and the ellipticity drop to zero, indicating that the $NiPt_3$ alloy film is paramagnetic at room temperature. This result is in accord with the previous reports that the onset point of ferromagnetism in Ni-Pt alloys at room temperature is about 42% of Ni [20–22]. Figure 2 shows that the variation trend of T_C of the $(Co_{1-x}Ni_x)Pt_3$ alloy films with the Ni content is similar to that of θ_K: T_C decreases monotonously with increasing Ni content and the decrease is more rapid when x is beyond 0.33. However, the magnitude of the decrease of T_C is larger than that of θ_K. At $x = 0$, $T_C = 273$ °C. At $x = 0.33$, T_C decreases to 233 °C, which is near to the practical disk writing temperatures attainable with low-cost laser sources.

Figure 3 shows the polar Kerr hysteresis loops of the above five $(Co_{1-x}Ni_x)Pt_3$ alloy films. It is seen that the films with $x = 0, 0.25$, and 0.33 exhibit a rectangular

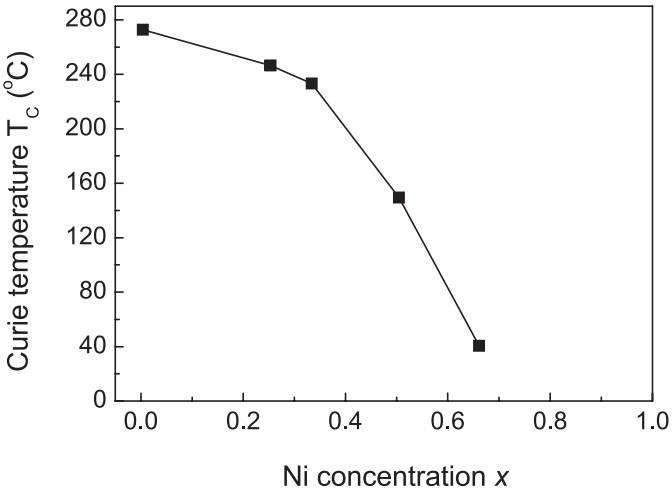

Fig. 2. The variation of Curie temperature as a function of Ni concentration in the $(Co_{1-x}Ni_x)Pt_3$ alloy films.

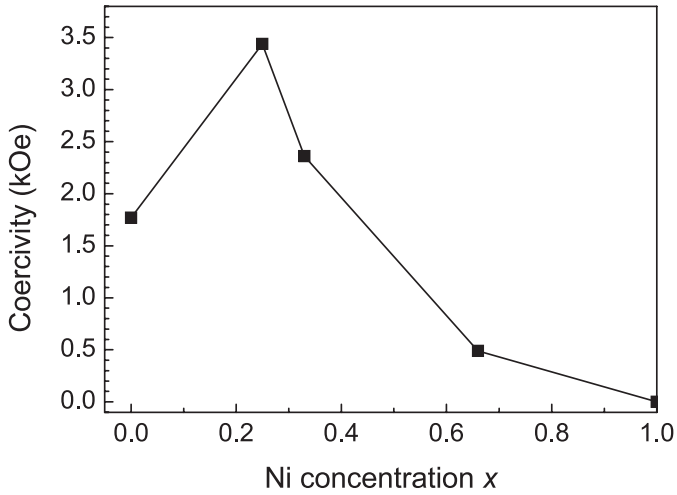

Fig. 4. The variation of coercivity as a function of Ni concentration in the $(Co_{1-x}Ni_x)Pt_3$ alloy films.

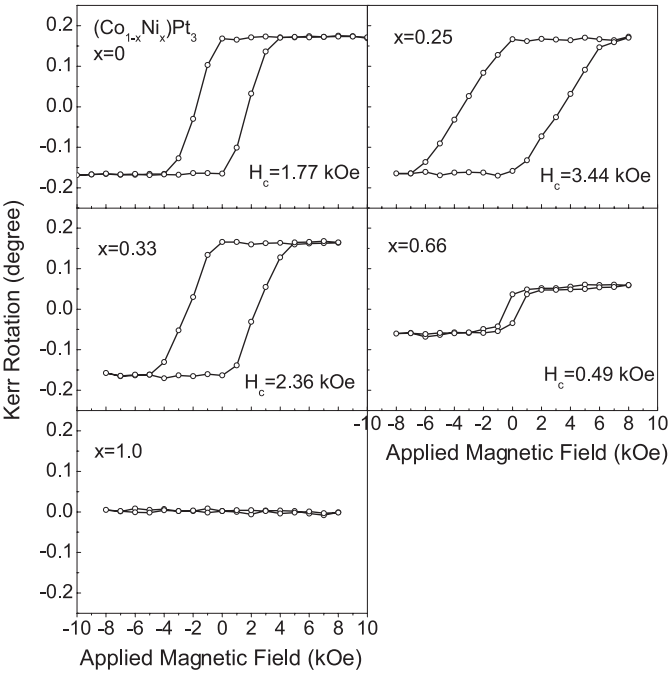

Fig. 3. Polar Kerr hysteresis loops of the $(Co_{1-x}Ni_x)Pt_3$ alloy films with different Ni contents: $x = 0, 0.25, 0.33, 0.66$, and 1.

hysteresis loop with a remanence ratio of near one, and their coercivities are 1.77, 3.44, and 2.36 kOe, respectively. These results indicate that the substitution of Ni for Co in the $CoPt_3$ alloy film with an atomic ratio of less than 33% can hold a strong PMA and a high coercivity while depressing the Curie temperature significantly. At $x = 0.66$, the film shows a degraded narrow hysteresis loop with a remanence ratio of about 50% and a coercivity of 0.49 kOe, indicating that the easy axis of magnetization shifts away from the perpendicular direction and inclines to the film plane. At $x = 1$, there is no polar Kerr signals present, indicating further that the $NiPt_3$ alloy film is paramagnetic at room temperature. The variation of coercivity with the Ni content is summed up and plotted in Figure 4.

In the ordered $(Co_{1-x}Ni_x)Pt_3$ pseudobinary alloy with a Cu_3Au-type ($L1_2$) structure, the Co and Ni atoms are randomly distributed on the corner sites of the fcc unit cell and Pt atoms occupy the fcc sites. Thus Co and Ni atoms, which are mainly responsible for the magnetism, are in position of second (and third) nearest neighbors having 12 Pt atoms in their shell of first neighbors [23]. However, in the corresponding disordered alloy, which is usually formed at low temperature, the magnetic and non-magnetic atoms randomly occupy the corner and fcc sites, and the direct exchange interaction between the magnetic atoms in position of first nearest neighbors leads to a higher Curie temperature than that of the ordered phase. In addition, the Curie temperature of thin film is generally lower than that of its bulk counterpart. In the case of $CoPt_3$, the homogeneous disordered alloy has a Curie temperature of 210 °C, which is 170 °C higher than that of the ordered one [24]. Here, the measured Curie temperature for the $CoPt_3$ film is 273 °C, which is much higher than 210 °C, indicating that the sputtered $CoPt_3$ alloy film here is disordered and inhomogeneous. This is consistent with the fact that the film is deposited under a substrate temperature much lower than the order-disorder transition temperature of 685 °C for the $CoPt_3$ alloy [10] and no ordering process has been involved. Because both the ordered $L1_2$ phase and disordered phase of $CoPt_3$ have cubic symmetry, the uniaxial magnetic anisotropy would not be expected in the homogeneous $CoPt_3$ alloy films. The occurrence of strong PMA in the above $(Co_{1-x}Ni_x)Pt_3$ alloy films further indicates that these films have a chemical structure anisotropy at least in a microscale. Previous studies also indicated that it is possible to form an alternating (111) Pt-rich and Co-rich planar local regions in the $CoPt_3$ alloy film during growth, due to the Pt segregation effect allowed by a dominant surface diffusion compared to bulk diffusion at a proper growth temperature. Such a chemical structure

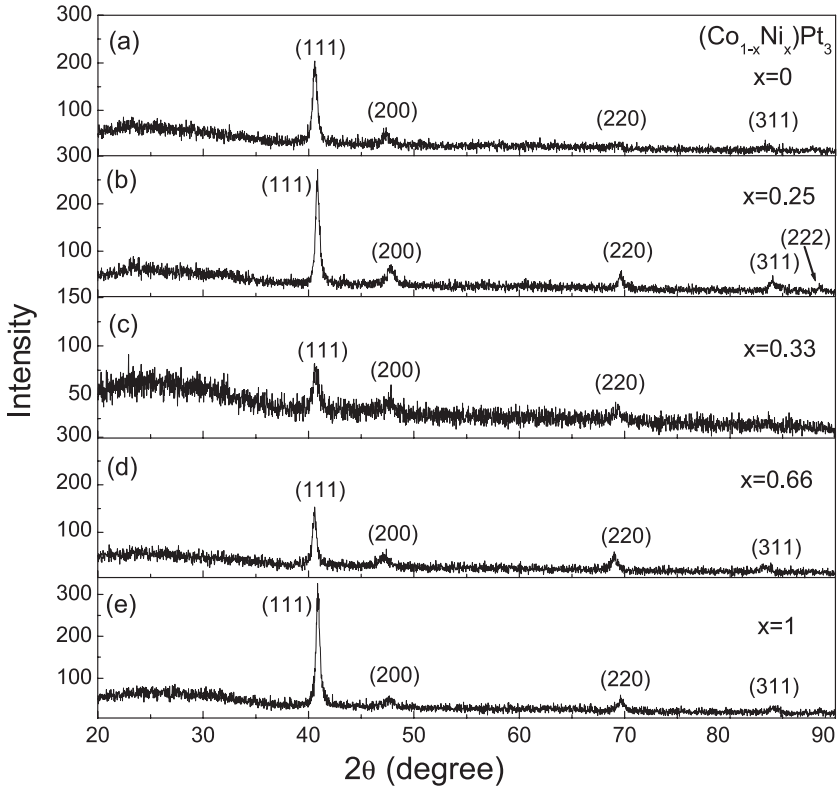

Fig. 5. X-ray diffraction patterns of the $(Co_{1-x}Ni_x)Pt_3$ alloy films with different Ni contents: $x = 0, 0.25, 0.33, 0.66$, and 1.

anisotropy similar to the Pt/Co multilayers is the origin of the large PMA in these alloy films [7,24].

Figure 5 shows the X-ray diffraction patterns of the $(Co_{1-x}Ni_x)Pt_3$ alloy films with $x = 0, 0.25, 0.33, 0.66$, and 1 in a range of 2θ from 20° to 90°. It is seen that all films are in a crystalline state, but no superlattice peaks, the evidence of long range ordering for the cubic $L1_2$ phase, can be found. At around $2\theta = 40.568, 47.336, 69.536$, and 83.336°, the $CoPt_3$ alloy film ($x = 0$) shows a strong (111) peak and several minor peaks which correspond to the (200), (220), and (311) reflections of the Co-Pt fcc phase, respectively, indicating that the film has a (111) preferred orientation normal to the film plane. The d spacing of the (111) peak is 2.222 Å, which is a little smaller than the d spacing 2.224 Å of the ordered $CoPt_3$. The full width at half maximum (FWHM) of the (111) peak $\Delta W = 0.4957°$ and the grain size estimated by the Scherrer's equation $D = 0.9\lambda/(\Delta W \cos\theta)$, where D is the diameter of the grain and λ is the wavelength of the X-ray [25], is 17.08 nm. With the addition of Ni at a small content, the (111) peak shifts to a higher 2θ and the peak becomes sharper and higher. For example, at $x = 0.25$, $2\theta = 40.856°$, corresponding to a d spacing of 2.207 Å, and $\Delta W = 0.432°$. The enhanced (111) peak height is possibly due to that Ni has a fcc crystal structure whereas Co has a hcp structure [13]. The decreased (111) d spacing can be attributed to the smaller atomic diameter of Ni than that of Co. The grain size of the $(Co_{0.75}Ni_{0.25})Pt_3$ film estimated by the Scherrer's equation is 19.62 nm. Generally speaking, a strong and sharp diffraction peak corresponds to a large grain size whereas a weak and broad diffraction peak corresponds to a small grain size. From Figure 5b we can see that the minor peaks are also strengthened and a (222) peak appears at $2\theta = 88.472°$, indicating that the lattice planes of the grains are developed with the growth of the grains. These results indicate that small content substitution of Ni for Co in the $CoPt_3$ alloy film can promote the growth of grains and improve the (111) orientation. However, when the Ni content x is increased to 0.33, the intensity of all diffraction peaks decreases greatly and the (111) peak is broadened and the corresponding grain size decreases to 13.62 nm, indicating that the growth of grains is hindered by the large content addition of Ni. With the further increase of Ni content, the film is in favor to form a fcc $NiPt_3$ structure. It can be seen that at $x = 0.66$, the (111) peak and the minor diffraction peaks become strong again and the grains grow up to 16.07 nm. At $x = 1$, the film exhibits a strong (111) texture and the grain size increases to 18.31 nm.

Because both the strain and the decrease of grain size can broaden XRD peaks, in order to verify the reasonableness of the grain sizes analyzed above, AFM was employed to measure the surface morphology of the $(Co_{1-x}Ni_x)Pt_3$ alloy films. The topography images of the films with $x = 0, 0.25, 0.33, 0.66$, and 1 are shown in Figure 6 and the measured grain sizes are 56.82, 79.36, 43.60, 42.37, and 68.97 nm, respectively. These values are about $3 \sim 4$ times larger than those estimated by the XRD. This is possible because the grain size estimated by the XRD is along the

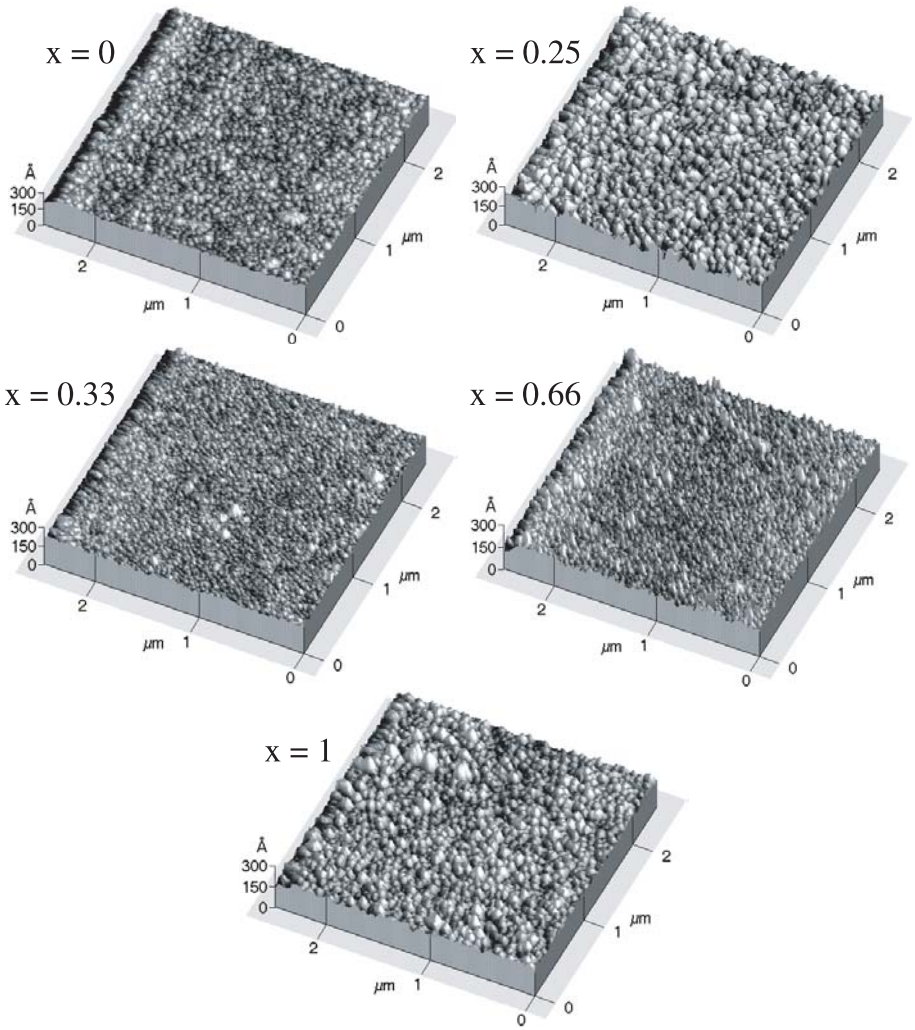

Fig. 6. AFM images with a scan size 2.5 μm $\times$2.5 μm for the $(Co_{1-x}Ni_x)Pt_3$ alloy films with different Ni contents: $x = 0, 0.25, 0.33, 0.66$, and 1.

direction perpendicular to the (111) face, whereas AFM gives indications about the in-plane grain size. In addition, the values measured by AFM are influenced by the sharp degree of the tip to some extent. In spite of this, the variation trend of the grain size with the Ni content measured by the XRD is in accord with that measured by the AFM qualitatively, verifying that the variation of width of the (111) peak is caused by the change of grain size. The root-mean-square surface roughnesses measured by AFM for these films are 9.03, 20.8, 8.01, 13.3, and 13.9 Å, respectively. The surface roughness of thin films is qualitatively related to the grain size. The smaller the grain size, the smoother the surface.

It was reported first that the strong PMA present in the evaporated Co-Pt alloy films was closely associated with the good (111) texture [4]. However, later investigations showed that the large PMA in the sputtered Co-Pt alloy films appeared to be independent of the (111) texture [26,27]. Comparing Figure 5 with Figure 3, we can see that the films with $x = 0, 0.25, 0.66$, and 1 show good (111) texture but only the former two films exhibit large PMA. On the other hand, the film with $x = 0.33$ shows the weakest (111) texture but a relatively large PMA. Hence, in the current case, the (111) preferred orientation is not correlated with the large PMA appeared in the $(Co_{1-x}Ni_x)Pt_3$ alloy films. It is well know that the coercivity H_c and the perpendicular anisotropy energy K_u are coupled each other and satisfy the Brown's relation:

$$H_c = 2\alpha K_u/M_s - N_{eff}M_s,$$

where α is a microstructure parameter related to the domain pinning, M_s is the saturated volume magnetization, and N_{eff} is the averaged local effective demagnetization factor [28,29]. Obviously, H_c increases with increasing K_u and is affected by the microstructure of the film such as grain size, surface roughness, growth orientation, and other metallographic factors. Similar to the PMA, in the current case the coercivity is not sensitive to the (111) orientation. However, on the whole, the coercivity increases (or decreases) with the increase (or decrease) of the grain size and surface roughness, as shown by Figures 4, 5 and 6 for $x = 0 \sim 0.66$. This is in accord with the conventional

domain wall mechanism: when the grain diameter is smaller than the domain size, a decrease in grain size will lead to a decrease in active volume of reversal domain and a decrease in surface roughness will lead to a decrease in domain-wall pinning, which both tend towards the decrease of coercivity.

4 Conclusions

Ni content dependence of the microstructure and magnetic and magneto-optical properties of the $(Co_{1-x}Ni_x)Pt_3$ alloy films has been investigated. On the whole, the addition of Ni to the $CoPt_3$ alloy film simultaneously decreases the Curie temperature T_C and Kerr rotation angle θ_K, but the decrease of T_C is more visible. When the Ni content x is less than 0.33, the decrease of θ_K is quite limited and the films still hold a strong PMA and a high coercivity, indicating that the alloy films can be used for the practical MO recording. Further increase of Ni content decreases the θ_K significantly and destroys the PMA. It is found that the addition of Ni with a small content will promote the growth of the grains and roughen the film surface and thus enhance the coercivity. Both the coercivity and PMA are not sensitive to the (111) preferred orientation.

This work is supported by the Chinese National Natural Science Foundation under Grant No. 10204015 and in part by of the Shanghai Science & Technology Development Foundation under Grant No. 02QA14026.

References

1. W.B. Zeper, F.J.A.M. Greidanus, P.F. Carcia, C.R. Fincher, J. Appl. Phys. **65**, 4971 (1989)
2. N. Nakajima, T. Koide, T. Shidara, H. Miyauchi, H. Fukutani, A. Fujimori, K. Iio, T. Katayama, M. Nyvlt, Y. Suzuki, Phys. Rev. Lett. **81**, 5229 (1998)
3. H. Zeng, M.L. Yan, N. Powers, D.J. Sellmyer, Appl. Phys. Lett. **80**, 2350 (2002)
4. C.-J. Lin, G.L. Gorman, Appl. Phys. Lett. **61**, 1600 (1992)
5. D. Weller, H. Brandle, G. Gorman, C.-J. Lin, H. Notarys, Appl. Phys. Lett. **61**, 2726 (1992)
6. M. Li, Z.H. Jiang, Z.Q. Zou, D.F. Shen, J. Magn. Magn. Mater. **176**, 331 (1997)
7. W. Grange, M. Maret, J.-P. Kappler, J. Vogel, A. Fontaine, F. Petroff, G. Krill, A. Rogalev, J. Goulon, M. Finazzi, N.B. Brookes, Phys. Rev. B **58**, 6298 (1998)
8. K. Xun, M. Li, J. Zhou, D.F. Shen, Thin Solid Films **347**, 253 (1999)
9. G. Srinivas, S.-C. Shin, Appl. Phys. Lett. **69**, 3086 (1996)
10. P.W. Rooney, A.L. Shapiro, M.Q. Tran, F. Hellman, Phys. Rev. Lett. **75**, 1843 (1995)
11. A.L. Shapiro, P.W. Rooney, M.Q. Tran, F. Heilman, J. Appl. Phys. **81**, 5053 (1997)
12. J.-G. Ha, K. Kyuno, R. Yamamoto, IEEE Trans. Magn. **33**, 1049 (1997)
13. S. Hashimoto, J. Appl. Phys. **75**, 438 (1994)
14. T. Shirakawa, K. Okamoto, K. Onishi, S. Matsushita, Y. Sakurai, IEEE Trans. Magn. MAG-**10**, 795 (1974)
15. J. Zhou, G.Q. Xia, K. Xun, Y.J. Zhang, S.Y. Liu, L.Y. Chen, D.F. Shen, Appl. Phys. A **70**, 453 (2000)
16. T.H. Kim, M.C. Cadeville, A. Dinia, Phys. Rev. B **53**, 221 (1996)
17. S. Basu, S.K. Ghatak, J. Magn. Magn. Mater. **123**, 97 (1993)
18. M. Mansuripur, M.F. Ruane, IEEE Trans. Magn. MAG-**22**, 33 (1986)
19. R. Hajjar, M. Mansuripur, IEEE Trans. Magn. MAG-**25**, 4021 (1989)
20. S.C. Shin, G. Srinivas, Y.S. Kim, M.G. Kim, Appl. Phys. Lett. **73**, 393 (1998)
21. M. Hansen, K. Andreiko, *Handbook of Binary Alloys* (McGraw-Hill, New York, 1985)
22. R.E. Parra, J.W. Cable, J. Appl. Phys. **50**, 7522 (1979)
23. T.H. Kim, M.C. Cadeville, A. Dinia, V. Pierron-Bohnes, H. Rakoto, Phys. Rev. B **54**, 3408 (1996)
24. M. Maret, M.C. Cadeville, A. Herr, R. Poinsot, E. Beaurepaire, S. Lefebvre, M. Bessiere, J. Magn. Magn. Mater. **191**, 61 (1999)
25. T.C. Huang, R. Savoy, R.F.C. Farrow, R.F. Marks, Appl. Phys. Lett. **62**, 1353 (1993)
26. J.-P. Hu, P. Lin, IEEE Trans. Magn. MAG-**32**, 4096 (1996)
27. T.A. Tyson, S.D. Conradson, R.F.C. Farrow, B.A. Jones, Phys. Rev. B **54**, R3702 (1996)
28. W.F. Brown, Rev. Mod. Phys. **17**, 15 (1945)
29. T. Suzuki, H. Notarys, D.C. Dobbertin, C.J. Lin, D. Weller, D.C. Miller, G. Gorman, IEEE Trans. Magn. MAG-**28**, 2754 (1992)